Lasers in Manufacturing Conference 2025

Microstructural Fracture Behaviour of PBF-LB/M Inconel 718 Components within different HIP Processes

David Sommer[a,*], Ben Truetsch[a], Cemal Esen[b], Ralf Hellmann[a]

[a]*Applied Laser and Photonics group, University of Applied Sciences Aschaffenburg, Wuerzburger Str. 45, 63743 Aschaffenburg, Germany*
[b]*Applied Laser Technologies, Ruhr University Bochum, Universitaetsstr. 150, 44801 Bochum, Germany*

Abstract

We report on a study of different hot isostatic pressing (HIP) cycles, improving the mechanical properties of additively manufactured Inconel 718 components. For this, PBF-LB/M built components are post-processed by different HIP sequences, as gas pressure and processing time are varied, leading to differences in microstructure and material characteristics. Static and dynamic mechanical testing are performed, evaluating the changes in mechanical properties with particular focus on the ultimate tensile strength and endurance limit. Furthermore, metallographic analysis is employed to investigate the achieved density and microhardness. Microstructural analysis, showing the grain boundaries, is used to identify generated phases and precipitations of the material matrix. Moreover, the fracture behaviour is classified by grain deformation during mechanical testing. As the HIP leads to microstructural changes of Inconel 718 components, mechanical properties can be improved significantly, enhancing the ultimate tensile strength and simultaneously the endurance limit.

Keywords: Hot isostatic pressing; Fatigue Behaviour; Ultimate Tensile Strenght; Microstructure; Inconel 718 ;

1. Introduction

For the industrial application of newly manufactured components, the knowledge of mechanical properties is of upmost importance, as maximum applicable loads and life cycle duration is contingent on different material parameters. For additive manufacturing of metals, especially for Laser Powder Bed Fusion (PBF-LB/M), component properties depend sensitively on process parameters and powder characteristics and have thus to be carefully evaluated (Balbaa et al., 2020). Due to the laser-based process and the machining within a powder bed, thermodynamic mechanisms occur, affecting the components properties like porosity, hardness and subsequently the ultimate tensile strength (UTS) as well as the fatigue (Mooney et al., 2019). Using thermal post-processing, the material properties can be improved, as the achieved density and microhardness can be increased by solution treatments, hot isostatic pressing (HIP) and ageing cycles. As a result, the mechanical properties can be enhanced, as various studies show an increase of the UTS for a multitude of materials (Casati et al., 2016; Herzog et al., 2020; Tammas-Williams et al., 2016). However, dynamic properties, determining life cycle durations, are often neglected.

For the Ni-based superalloy Inconel 718 (IN718), combinations of solution and ageing treatments and HIP are used for a thermal post-processing, causing precipitations of different phases and associated changes in microstructure (Sahu et al., 2021; Qin et al., 2019). Within these, adjusted time-temperature sequences have to be employed to avoid precipitation of brittle phases, diminishing material properties (Gao et al., 2019).

Against this background, we report on a study of different HIP cycles for the optimization of static and dynamic mechanical load behaviour. For this, processing parameters like sustain temperature and gas pressure are varied during HIP, subsequently evaluating the UTS and the different regimes of fatigue for the components. Differences in mechanical properties are investigated, discussing material properties like achieved density and microhardness. Furthermore, microstructural changes are analysed, identifying different precipitations during the heat treatment and microstructural properties within plastic deformation.

2. Materials and Methods

For the additive manufacturing of the IN718 components, a Lumex Avance-25 (Matsuura, Fukui, Japan) is used, performing the PBF-LB/M process with a Laser power P_L = 320 W, a scan-speed of v_c = 240 mm/min, a hatch distance of d_h = 140 µm and a layer height of h_l = 50 µm. Standard tensile specimens are manufactured vertically for the evaluation of mechanical properties as well as cubic samples are fabricated for metallographic analysis.

Thermal post-processing is performed according to Tab. 1. At first, for all cycles, a Solution Treatment (ST) is performed as well as after HIP, a Double Ageing (DA) procedure follows. During the HIP, gas pressure and sustain time are varied in different process sequences, maintaining the temperature.

For the static testing, a universal testing machine AG-Xplus (Shimadzu, Kyoto, Japan) is used, evaluating the Ultimate Tensile Strength (UTS) with a maximum applicable load of F_{max} = 50 kN for a batch of three specimens for the different states of material. Dynamic testing is performed with a linear electrodynamic testing machine UD020 (Step Engineering, Resana, Italy), applying a sinusoidal oscillation with a frequency of f = 100 Hz and a maximum amplitude of F_{max} = 14 kN. As the different regimes of fatigue are evaluated within a Wöhler-curve, a multitude of loads is tested, and the endurance limit is determined by the staircase-method.

Table 1: Temperature-Time sequences for the different HIP cycles

	ST	HIP	DA
as-built	----	----	----
HT 1	1065 °C / 90 min	1150 °C / 3h / 175 MPa	720 °C / 8 h, 620 °C / 10 h
HT 2	1065 °C / 90 min	1150 °C / 4h / 175 MPa	----
HT 3	1065 °C / 90 min	1150 °C / 4h / 150 MPa	720 °C / 8 h, 620 °C / 10 h
HT 4	1065 °C / 90 min	1150 °C / 4h / 175 MPa	720 °C / 8 h, 620 °C / 10 h
HT 5	1065 °C / 90 min	1150 °C / 5h / 175 MPa	720 °C / 8 h, 620 °C / 10 h

3. Results and Discussion

The static testing of the tensile components shows very differing behaviour for the conducted heat treatments, as depicted in Fig. 1. At first, the as-built state of IN718 shows a ductile tensile behaviour and an UTS of R_m = 845 MPa. Due to high cooling rates during the PBF-LB/M process, a very fine-grained microstructure develops, promoting a ductile material structure and reaching a microhardness of 307 HV10. Next, the HT 2, only performing a ST and HIP without an ageing procedure afterwards, leads to a high increase in strain, as the ductile structure is immensely intensified by a homogenization of the material structure. Subsequently, the hardness is reduced to 191 HV10.

Contrary to this, heat treatments with a following DA procedure lead to a significant improvement of the UTS, as shown in Fig. 1. With maximum load capacities of 1120 to 1186 MPa, an increase of minimum 275 MPa or about 33 % is achieved. Furthermore, for all specimens, the necking zone is completely excluded, as a more brittle, but strong material is generated by the combination of ST, HIP and DA. Due to the generation of γ′- and γ″-precipitations, the material structure is strengthened significantly, enhancing microhardness for the heat-treated components strongly in comparison to as-built parts. As depicted in Tab. 2, the microhardness ranges between 454 HV10 and 495 HV10, showing a minimum improvement of 147 HV10.

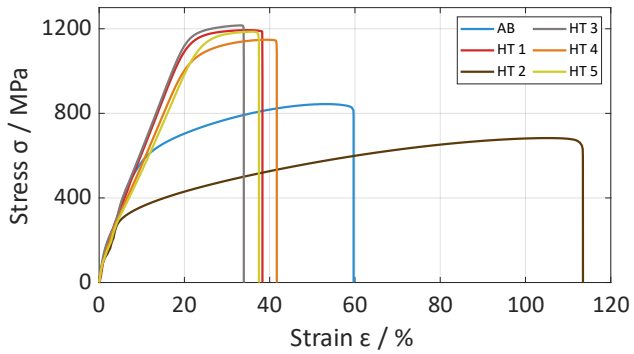

Figure 1: Comparison of as-built and heat-treated components, evaluating the UTS with a Stress-Strain diagram

Within the investigation of dynamic mechanical properties, the effect of sustain time of the HIP process is examined with the comparison of the HT1, HT4 and HT5 with the as-built state of the IN718. As shown in the Wöhler-diagram in Fig. 2, the as-built state shows a long Low Cycle Fatigue (LCF) regime, merging into the High Cycle Fatigue (HCF) regime, rapidly decreasing the number of performed cycles, as the Wöhler-line is determined by the gradient k = 2.97. Finally, the endurance limit can be defined at σ_{ED} = 85 MPa. For the heat-treated samples, differences in the LCF regime can be detected, as the transition into the HCF regime can be determined at very different cycle numbers, as shown in Fig. 2. During the HCF, an increase develops, as the Wöhler-lines are described by k = 4.67 (HT1), k = 4.06 (HT4), and k = 5.80 (HT5), leading to an intersection of the Wöhler-line of the as-built components. For the endurance limit a significant improvement is shown, as the endurance limits can be set to σ_{ED} = 175 MPa (HT1), σ_{ED} = 185 MPa (HT4), and σ_{ED} = 200 MPa (HT5).

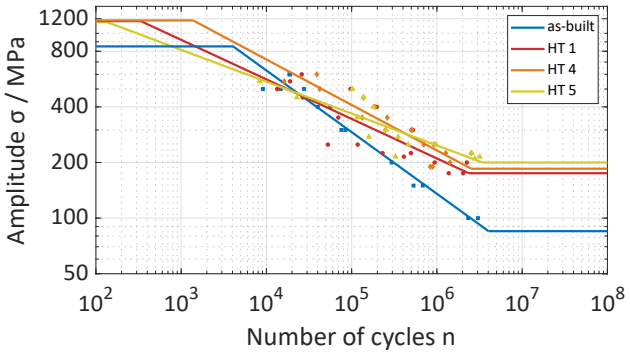

Figure 2: Wöhler diagram for the as-built and heat-treated components, evaluating the different regimes of fatigue

For the mechanical properties, especially the fatigue behaviour, porosity and material structure are of upmost importance, as the UTS and the endurance limit are highly affected. As listed in Tab. 1, the as-built state of IN718 shows a density of 99.16 %, as gas inclusions and melting properties lead to process induced porosities between 0.2 – 1.8 % (Becker et al., 2016, Balbaa et al., 2020). During the HIP, the isostatically applied gas pressure in combination with diffusion mechanisms lead to a reduction of porosities. As listed in Tab. 2, the different heat treatments lead to a significant improvement of the density, as it ranges between 99.94 – 99.97 %.

Table 2: Summary of metallographic and mechanical properties of heat-treated components

	HV10	ρ / %	R_m / MPa	σ_{ED} / MPa
as-built	307	99.16	845	85
HT 1	455	99.97	1181	175
HT 2	191	99.94	681	-----
HT 3	465	99.96	1177	-----
HT 4	454	99.94	1205	185
HT 5	495	99.95	1167	200

Furthermore, the material structure of the HIP components varies, as heat treatments cause phase precipitations and grain boundary movements. For the as-built state, the microstructural investigation shows the primary and secondary microstructure, as the melting paths and signs of grain boundaries are visible (cf. Fig. 3a). The melting paths are shown by segregation patterns, developing at the transition area, as well as a fine-grained microstructure is visible. The fine-grained structure originates from the high cooling rate of the components during the PBF-LB/M process, encouraging a ductile tensile behaviour. For the HIP, the microstructure differs basically, as different precipitations are identified (cf. Fig. 3b-d). Due to the applied temperatures, a migration of grain boundaries is enabled, getting reinforced by diffusion mechanisms. Subsequently, δ-phases precipitate at the grain boundaries, not completely dissolving during the HIP process (Gao et al, 2019). Though, a homogenization of the material structure in caused by ST and HIP, increasing fatigue performance. Additionally, the DA procedure develops γ‘- and γ‘‘-precipitations, improving the static mechanical load behaviour, as the material structure is strengthened.

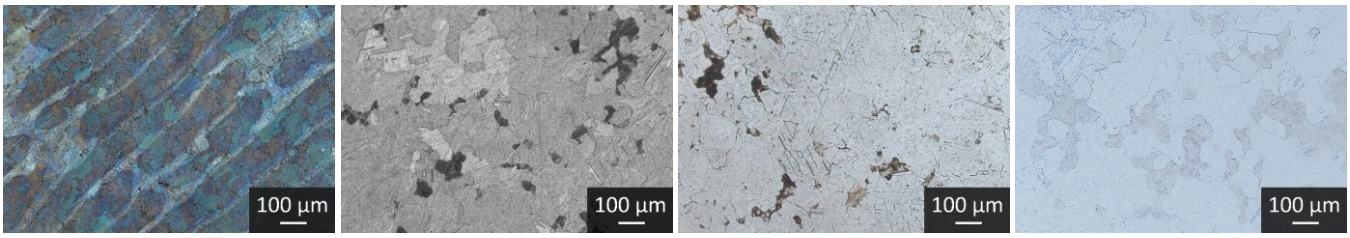

(a) (b) (c) (d)

Figure 3: Microscope images of etched components of the a) as-built, b) HT 3, c) HT 4, and d) HT 6 state, showing microstructural differences

During the static testing, a plastic deformation of the components is forced for the evaluation of the UTS. Within this, microstructural deformations occur, as depicted in the microstructural analysis of a standard tensile specimen in Fig. 4. The grain boundaries are dislocated by the applied stress, forming elongated grains in the direction of the load application (cf. Fig. 4b). While the high dislocation activity of the γ-matrix leads to a deformation of the microstructure, higher applied stress can initiate crack points in the δ-phase, developing intra-granular breakages (Nayan et al., 2015). Furthermore, shear bands develop during plastic deformation, as depicted in Fig. 4b. Dislocations in the γ-matrix show movements in subsequence to the applied load, causing the shear bands in misalignment of 45° in regard to the direction of the applied stress, as the maximum shear stress is determined with this stress tensor (Zhang et al., 2015).

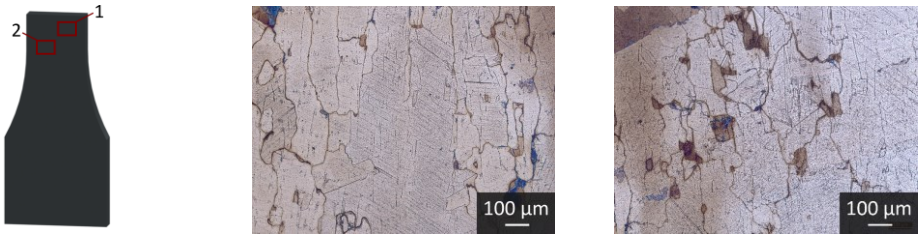

(a) (b) (c)

Figure 4: Microstructural deformation of HT 4 components, showing a) schematic depiction of the measured zones, b) elongated grains (zone 1), and c) shear bands as a consequence of plastic deformation (zone 2)

4. Conclusion

Within this study, we report on the mechanical properties and microstructural changes of PBF-LB/M built IN718 components with post-processed heat treatments. For this, different HIP cycles are conducted, varying the processing sequence and HIP parameters like sustain time and gas pressure. Static and dynamic mechanical properties are tested, evaluating the UTS and the endurance limit for the different components in comparison to the as-built state of IN718. The UTS is increased significantly by HIP in combination with a double-ageing sequence, as the precipitation of γ‘-phases and γ‘‘-phases lead to an increase in microhardness and an improved static load behaviour, summarized in Tab. 2. Furthermore, the dynamic testing shows an increase of the endurance limit from 175 MPa to 200 MPa for HIP-cycles. Due to the applied gas pressure during the high temperature heat treatment, the density can be raised as well as different phase precipitations lead to enhanced fatigue behaviour. As shown in the microstructural analyses, a grain growth and the development of γ’- and γ‘‘-precipitations as well as the δ-phase leads to a homogenization of the microstructure and an improvement in mechanical properties. Additionally, the microstructural changes in succession to mechanical stress are shown, as an elongation of the grain structure and shear bands can be observed.

References

Balbaa, M.; Mekhiel, S.; Elbestawi, M.; McIsaac, J.; 2020. On selective laser melting of Inconel 718: Densification, surface roughness, and residual stresses, Materials & Design, 193, S. 108818. doi: 10.1016/j.matdes.2020.108818.

Becker H.; Dimitrov, D.; 2016. The achievable mechanical properties of SLM produced Maraging Steel 300 components, Rapid Prototyping Journal, 22 (3), S. 487-494. doi: 10.1108/RPJ-08-2014-0096.

Casati, R.; Lemke, J.; Tuissi, A.; Vedani, M.; 2016. Aging Behaviour and Mechanical Performance of 18-Ni 300 Steel Processed by Selective Laser Melting, Metals, 6 (9), S. 218. doi: 10.3390/met6090218.

Gao, Y.; Zhang, D.; Cao, M.; Chen, R.; Feng, Z.; Poprawe, R.; Schleifenbaum, J.H.; Ziegler, S.; 2019. Effect of delta phase on high temperature mechanical performances of Inconel 718 fabricated with SLM process, Materials Science and Engineering: A, 767, S. 138327. doi: 10.1016/j.msea.2019.138327.

Herzog, D.; Bartsch, K.; Bossen, B.; 2020. Productivity optimization of laser powder bed fusion by hot isostatic pressing, Additive Manufacturing, 36, S. 101494. doi: 10.1016/j.addma.2020.101494.

Mooney, B.; Kourousis, K.I.; Raghavendra, R.; Agius, D.; 2019. Process phenomena influencing the tensile and anisotropic characteristics of additively manufactured maraging steel, Materials Science and Engineering: A, 745, S. 115–125. doi: 10.1016/j.msea.2018.12.070.

Nayan, N.; Gurao, N.P.; Narayana Murty, S.; Jha, A.K.; Pant, B.; George, K.M.; 2015. Microstructure and micro-texture evolution during large strain deformation of Inconel alloy IN718, Materials Characterization, 110, S. 236–241. doi: 10.1016/j.matchar.2015.10.027.

Qin, S.; Herzog, S.; Kaletsch, A.; Broeckmann, C.; 2019. Effects of HIP on microstructure and creep properties of Inconel 718 fabricated by laser powder-bed fusion, Europe's Annual Powder Metallurgy Congress and Exhibition. doi: 10.18154/RWTH-2022-03976.

Sahu, A.K.; Bag, S.; 2021. Design of a double aging treatment for the improvement of mechanical and microstructural properties of pulse micro-plasma arc welded alloy 718, Journal of Materials Science, 56 (23), S. 13400–13415. doi: 10.1007/s10853-021-06121-8.

Tammas-Williams, S.; Withers, P.J.; Todd, I.; Prangnell, P.B.; 2016. The Effectiveness of Hot Isostatic Pressing for Closing Porosity in Titanium Parts Manufactured by Selective Electron Beam Melting, Metall Mater Trans A, 47 (5), S. 1939–1946. doi: 10.1007/s11661-016-3429-3.

Zhang, H.; Zhang, K.; Zhou, H.; Lu, Z.; Zhao, C.; Yang, X.; 2015. Effect of strain rate on microstructure evolution of a nickel-based superalloy during hot deformation, Materials & Design, 80, S. 51–62. doi: 10.1016/j.matdes.2015.05.004.